J. Phys. B: At. Mol. Opt. Phys. **31** (1998) 2381–2394. Printed in the UK PII: S0953-4075(98)89212-2

Electron-impact ionization of Mg

R F Boivin† and S K Srivastava

Jet Propulsion Laboratory, California Institute of Technology, 4800 Oak Grove Drive, Pasadena, CA, 91109-8099, USA

Received 13 November 1997, in final form 23 March 1998

Abstract. A crossed beam technique is used to measure ionization cross sections of metallic atoms. Relative values of cross sections of single, double and triple ionization of magnesium have been successfully measured over the 0–700 eV range with an estimated accuracy of 11%, 19% and 25%, respectively. Absolute values of cross sections have been obtained by normalization to a theoretical value at high electron energy. The theoretical value is calculated by using the generalized oscillator strength approximation. Results are compared to previously published values and, for single ionization in particular, a comparison with theoretical cross sections is performed.

1. Introduction

Most astrophysical plasmas are in non-local thermal equilibrium (LTE) (see, for instance, Shull 1982, Raymond 1977) and require a vast variety of atomic data for modelling purposes. In particular, ionization rates for various atomic species found in astrophysical plasmas are of great importance. In the past, Lotz (1967) classical-empirical formula has been extensively used to calculate ionization rates. However, recent measurements and improved theoretical calculations clearly indicate that Lotz rates are not accurate and may be in error by as much as a factor of 3. Arnaud and Rothenflug (1985) have improved this situation and generated ionization cross sections for 15 elements. Generally there is agreement with previous results. However, for metal atoms the situation is still far from being satisfactory.

Experimental determination of ionization cross sections for metal atoms is not an easy task due to several difficulties. First, most metal atoms require high temperatures to form their vapours. Second, in order to obtain cross section values, absolute number densities in vapour phase are needed. Therefore, these cross sections have been measured only by very few experimental groups and for a limited number of elements. Mg is among that select list. It is an astrophysically important atom since its emission spectra have been recorded by several ground-based and spacecraft-based instruments (Shull 1985, Jefferies 1991). Mg emission was also observed immediately following the entry of the Shoemaker–Levy 9 comet into the Jovian atmosphere (Feldman 1996). In the seventies, Vainshtein *et al* (1972), Okudaira *et al* (1970), Okuno *et al* (1970) and Karstensen and Schneider (1975, 1978) measured the electron-impact ionization cross section for Mg. More recently Freund *et al* (1991) and McCallion *et al* (1992) have published cross section values for Mg. On the theoretical front, Peach (1966, 1970) has calculated ionization cross section for the Mg atom using a number of theoretical models such as the Coulomb–Born, Born-exchange, Born–Ochkur and modified Coulomb–Born approximations. McGuire (1977)

† NRC-NASA Resident Research Associate.

0953-4075/98/102381+14$19.50

used the generalized oscillator strength approximation to calculate the single-ionization cross section for Mg. The emerging picture in terms of cross section for Mg is becoming clearer, however, a great spread in cross section values still exists. The accuracy and validity of the new experimental data is subject to confirmation by other groups which could use different experimental techniques for cross section measurements. Thus, for all the reasons mentioned above, we have chosen Mg as our first metal atom for ionization cross section measurement.

2. Experimental approach

2.1. Experimental apparatus

A detailed description of the experimental arrangement has been discussed in earlier publications (Trajmar *et al* 1977, Krishnakumar and Srivastava 1988) and only a brief description of the main features will be presented here. The experimental apparatus can be separated into three major components: the electron beam system, the extraction/detection system and the metal beam generator. A schematic diagram of the experimental apparatus is shown in figure 1.

2.1.1. Electron beam system. A three element pulsed electron gun (Khakoo and Srivastava 1984) is used to generate the electron beam. A pulse generator provides pulses of 100 ns duration every 10 ms to the electron gun optics. A Faraday cup is used to monitor the current during the experiment (typically $\sim$2 mA). The energy of the electrons is continously varied from 0 to 690 V. The current intensity remains constant for the entire energy range. The electron beam diameter is estimated to be less than 1 mm (inferred from the burnt spot on the Faraday cup surface). The electrons go through an open solenoid where they intersect the Mg metal beam (figure 1 #8) at a right angle. The collimating magnetic field inside the solenoid is maintained at 100 mG. For calibration purpose, a gas capillary (figure 1 #11) is also mounted perpendicularly above the electron beam. The capillary extremity is coaxial with the crucible aperture, thus forming a beam of atoms at right angles to the electron beam. Pressure inside the vacuum chamber is kept at about 1×10^{-7} Torr during the Mg emission. Electron beam energy is calibrated by measuring the ionization threshold of Xe which is accurately known (Rosenstock *et al* 1977). A correction of about 1 eV is found for misaligned filament and contact potential effects.

2.1.2. Extraction/detection system. Immediately after every electron pulse ($\sim$100 ns), a second pulse generator (triggered by the first) provides an extraction pulse to the extraction grids (figure 1 #10). The ion extraction field is produced by the application of pulses of about 40 V in amplitude and about 1 μs in duration between a pair of extraction grids located on each side of the beam intersection region. Optimization of amplitude, duration and delay parameters for the extraction pulses was performed to ensure that the maximum of the newly formed ions were collected. The ions were then collected and focused at the entrance of the mass spectrometer (figure 1 #13) through a series of electrostatic lenses (figure 1 #12). A channeltron particle detector (figure 1 #14) was used to count each collected ion. The multichannel analyser accumulated and stored data in 1024 channels. The extraction/detection system can be used in two distinct modes: single mass detection and mass spectrum detection. In the single mass detection mode, the spectrometer is tuned to a specific mass and the electron energy is varied from 0 to 690 V. The 0–690 V cycle is repeated until sufficient counts are accumulated on all channels. Energy resolution is

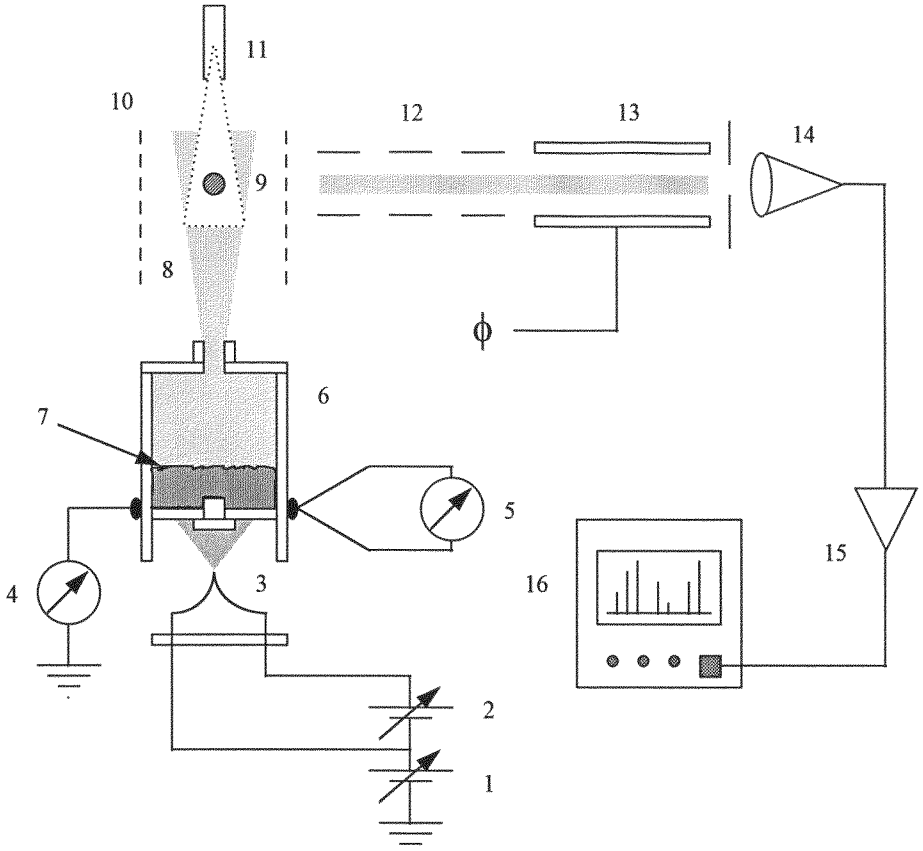

Figure 1. Schematic diagram of the experimental apparatus. (1) High voltage power supply, (2) high current power supply, (3) tungsten filament, (4) emission current meter, (5) thermocouple, (6) crucible, (7) metallic powder, (8) metal beam, (9) electron beam, (10) extraction grids, (11) gas capillary, (12) enzel lenses, (13) quadrupole mass analyser, (14) detector, (15) amplifier and (16) multichannel analyser.

0.67 V per channel. The extraction system is also being used in the mass spectrum mode. In this mode the electron energy is fixed and the mass spectrometer is scanned to obtain the mass spectrum. Mass resolution is about 0.1 amu per channel.

2.1.3. Metal beam source. The metal beam source consisted of a molybdenum crucible (figure 1 #6) filled with a 99.8% pure Mg powder (Goodfellow 1997). The cylindrical shaped crucible is terminated by a small tube (0.79 mm long) with an inner diameter of 0.123 mm, from which the vaporized Mg escaped to form the metal beam. In the intersection region , the diameter of the Mg beam was estimated to be about 4 mm (measured by triangulation from the Mg deposition surface located on the base of the capillary holder). A tungsten filament (figure 1 #3) was placed underneath the crucible. The filament was slowly brought to a potential of about 900 V with respect to the ground. A current of a few amperes was circulated through the filament. The emission current was used to heat the crucible and consequently vaporize the Mg powder (figure 1 #7). A platinum–rhodium thermocouple (figure 1 #5) was used to measure the temperature of the crucible. The temperature range

for Mg vaporization was observed to be between 425 and 500 °C. These temperatures correspond to Mg vapour pressures of 1×10^{-2} and 1×10^{-1} Torr inside the crucible, respectively (Weast 1983a).

2.2. Ionization efficiency curves and normalization

The ionization efficiency curves showing the variation of the relative ion intensity as a function of the electron impact energy for the various Mg ions were obtained under the following conditions.

(1) Stable electron beam current. The electron gun current did not change during all measurement.

(2) Constant ion extraction conditions. The conditions for ion extraction remained the same during all measurements (Mg, Xe and Ne (see section 3.2)).

(3) Constant crucible temperature. The crucible temperature remained constant (within ±10 °C) during each Mg ionization efficiency curve measurement.

(4) Mg^+ was the dominant ion in the extracted ion beam. Mg^+ was the highest peak in the mass spectrum during measurements.

(5) Frequent electron energy calibration. After each ionization curve measurement, electron energy calibration was performed by measuring the threshold voltage for the ionization of Xe.

(6) Verification of the extraction system. The Xe ionization efficiency curve was measured immediately after every measurement of Mg ionization efficiency curve. Shape agreement between Xe curves and the previously published cross section (Krishnakumar and Srivastava 1988) was within 3%.

(7) Statistics. The number of counts per channel was such that the error associated with random statistical noise was negligible (noise counts corresponded to 0.03% of total count for single ionization and to 1% of total count for triple ionization).

The ionization efficiency curves represent the variation of the ion formation intensity as a function of electron impact energy. In the crossed electron–atomic beam mode, the ion intensity $I(E)$ is related to the ionization cross section $\sigma(E)$ by the following expression (Brinkman and Trajmar 1981, Dunn 1985):

$$I(E) = K(m)\sigma(E) \int_v \rho(\boldsymbol{r}) f_e(\boldsymbol{r}, E) \Delta\Omega(\boldsymbol{r}) \, \mathrm{d}\boldsymbol{r} \tag{1}$$

where $I(E)$ is the number of ions detected per second as a function of incident electron energy E, $K(m)$ is an ion-mass-dependent factor which includes the combined efficiency of transmission of ions through the extraction grids, ion optics and quadrupole mass analyser and the detection efficiency of the charged particle detector. The $\rho(\boldsymbol{r})$, $f_e(\boldsymbol{r}, E)$ and $\Delta\Omega(\boldsymbol{r})$ functions are the target density, the spatial electron flux distribution and the solid angle of detection for a collision point located at $\boldsymbol{r}$ within the intersection volume of the two beams, respectively. If we assume that the spatial electron flux distribution is independent of the incident electron energy, and considering the special case of the Mg metal beam, equation (1) can be written as:

$$I_{Mg^+}(E) = K(m_{Mg^+}) G_{Mg} \sigma_{Mg^+}(E) \tag{2}$$

where $K(m_{Mg^+})$ is the combined transmission–detection factor for the singly charged Mg ion, G_{Mg} is a geometric function related to target density, solid angle of detection and electron spatial distribution, and $\sigma_{Mg^+}(E)$ is the ionization cross section for the production of singly ionized Mg. According to equation (2), the ion intensity $I_{Mg^+}(E)$ is directly proportional to the ionization cross section. Thus, the ion intensity $I_{Mg^+}(E)$ and a single

absolute value of the cross section is all that is needed to obtain the complete cross section function.

3. Results and discussion

3.1. Mass spectrum and ionization efficiency curve

The crucible is heated to a temperature where the Mg is detected by the mass spectrometer. The spectrometer is set to the mass spectrum mode and several mass spectra are recorded at different electron energies (25, 50, 75, 100, 200, 300, 400, 500 and 600 eV). Of particular interest are the mass spectra obtained at 25, 100 and 400 eV shown in figure 2. At 25 eV, apart from the usual vacuum contaminants (H_2O, CO and CO_2), only the singly ionized Mg is seen in the mass spectrum. This is because of the fact that the electron energy is too low to create doubly or triply ionized Mg. The Mg^+ secondary peaks (mass 25 and 26) are of course associated with the Mg isotopes which have 10 and 11% natural abundances, respectively (Weast 1983b). At 100 eV, both singly and doubly ionized Mg peaks are clearly visible. Note also, that the ratios of impurity intensities over the Mg^+ intensity are quite larger than in the previous spectrum. This is due to two factors: first and foremost, that the single ionization cross section for Mg is much larger at 25 eV than 100 eV (see section 3.2) and secondly, that for contaminants, the situation is reverse, H_2O and CO_2 ionization cross sections only reach their maxima at 120 and 110 eV, respectively (Rao *et al* 1995, Srivastava and Nguyên 1987). At 400 eV, singly, doubly and triply ionized Mg are present in the spectrum. Note also, that at this energy, the Mg^{2+} peak is now of the same order of magnitude as the singly ionized Mg peak. This situation translates for both species into comparable ionization cross section values at 400 eV. This subject will be discussed further in section 3.3.

The spectrometer is then set in the single-mass detection mode and single-, double- and triple-ionization efficiency curves are subsequently obtained as a function of electron impact energy. The single-ionization efficiency curve is normalized to obtain absolute values of the cross section. For normalization, we have chosen the cross section value calculated by McGuire (1977) using the generalized oscillator strength approximation at 500 eV. There are a number of reasons to justify this choice. First, McGuire's calculations at high electron impact energies have been shown to be quite reliable by Brooks *et al* (1978). Second, a different model based on a modified Coulomb–Born approximation (Peach 1970) yields exactly the same value for the cross section at this particular energy (see figure 3). Third, previous experimental results from two independent groups (Okudaira *et al* 1970, McCallion *et al* 1992) also converge toward this value of 6.50×10^{-17} cm^2 at 500 eV (see figure 4). Finally, in this electron energy range, the decrease of the cross section as a function of energy is slow and is independent of processes such as autoionization, transient negative ion and metastable excited atoms observed near threshold (Rosenstock *et al* 1977, Shafranyosh and Margitich 1996).

3.2. Single ionization cross section for Mg

Our experimental ionization efficiency curve is normalized and shown in figure 3. McGuire's (1977) cross section values are also shown in figure 3. The overall agreement between calculations and experiment is quite good. As expected, excellent agreement is found in the 300–500 eV range. However, our cross section value at maximum is 13% lower than the calculated cross section. Note also, that in the 60–250 eV range our cross section values

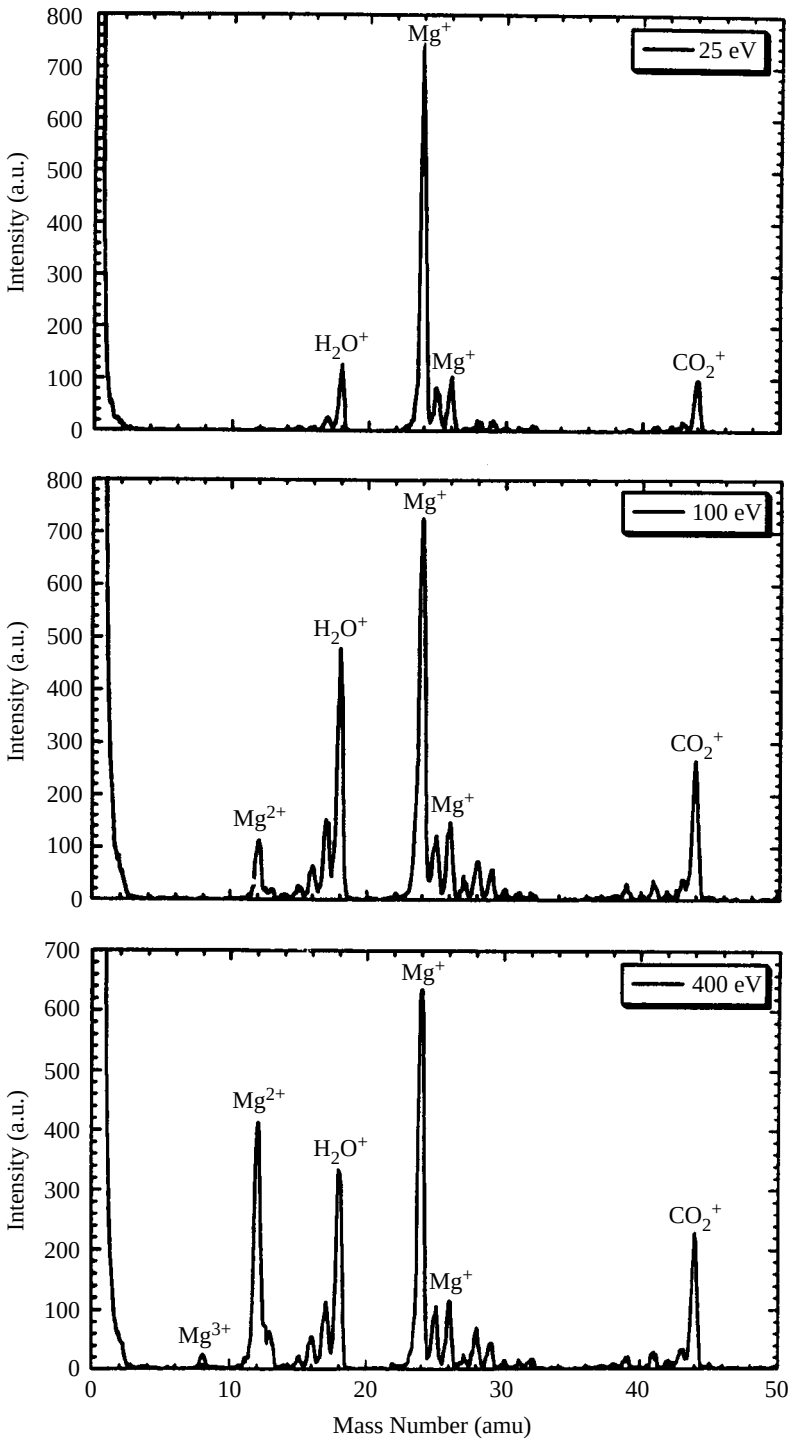

Figure 2. Mass spectra featuring Mg ions observed at different electron energies (25, 100, 400 eV).

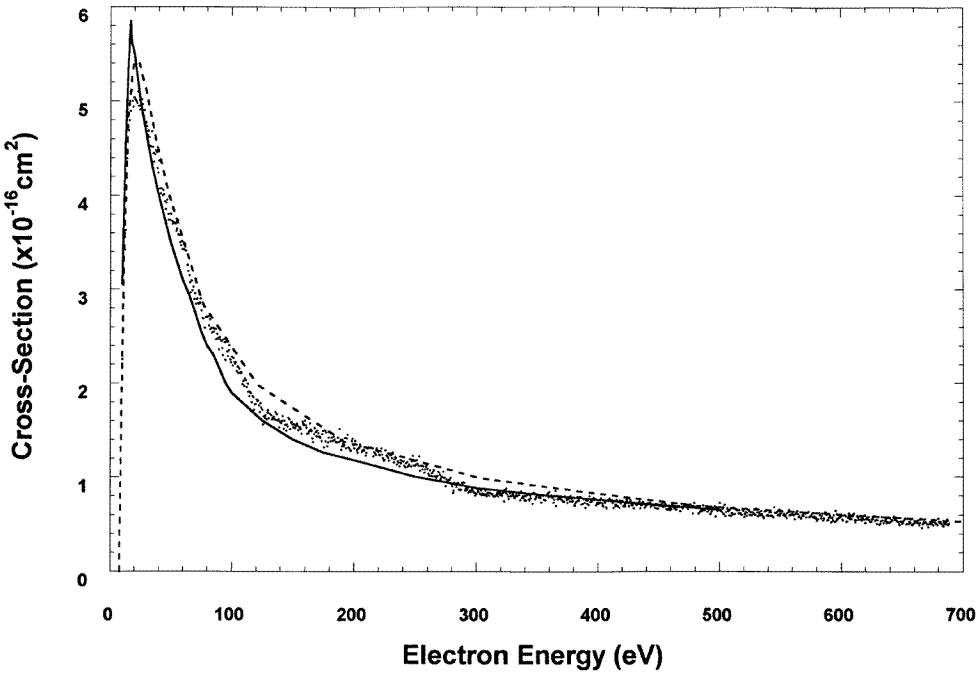

Figure 3. Single ionization cross section of Mg by electron impact. Theory: (——) McGuire (1977); (- - - -) Peach (1970); (· · · · · ·) present results.

are about 9% larger than those predicted by McGuire (1977). Calculated ionization cross sections for the Mg atom using a modified Coulomb–Born approximation (Peach 1970) are also shown in figure 3. This model takes into account inner shell contributions to the ionization cross section. The general agreement between the model and experiment is also very good. In this case, the maximum cross sections are only 5.4% apart, the calculated value being slightly larger. Excellent agreement (within 5% or less) is found in both the 40–120 eV and 400–700 eV ranges. In the 120–400 eV region, the calculated values are about 7% larger than the experimental cross sections. Note also, that for almost the entire energy range reported here the experimental data are located between the two theoretical cross section curves.

A curve fit was performed on our 1024 experimental cross section measurements, and this fit is shown in figure 4. From this fit, cross section values for specific electron impact energies were obtained and presented in table 1. All previous experiments featuring the measurement of single ionization of Mg are included in figure 4. The single-ionization cross sections measured by McCallion *et al* (1992) for energies up to 5.3 keV are compared to our experimental results. Excellent agreement is found throughout our entire energy range. However, their maximum cross section value is 7% higher than ours and their cross sections values in the 450–700 eV range are about 16% lower than our cross sections. Cross sections measured by Freund *et al* (1990) for energies up to 200 eV are also in good agreement with our experimental values. Their maximum cross section is less than 4% higher than ours while their cross sections in the 100–200 eV range are about 10% higher than ours. Note that McCallion *et al* (1992) have used Freund *et al* (1990) cross sections in the 20–40 eV range to normalize their ionization efficiency curve. Cross sections

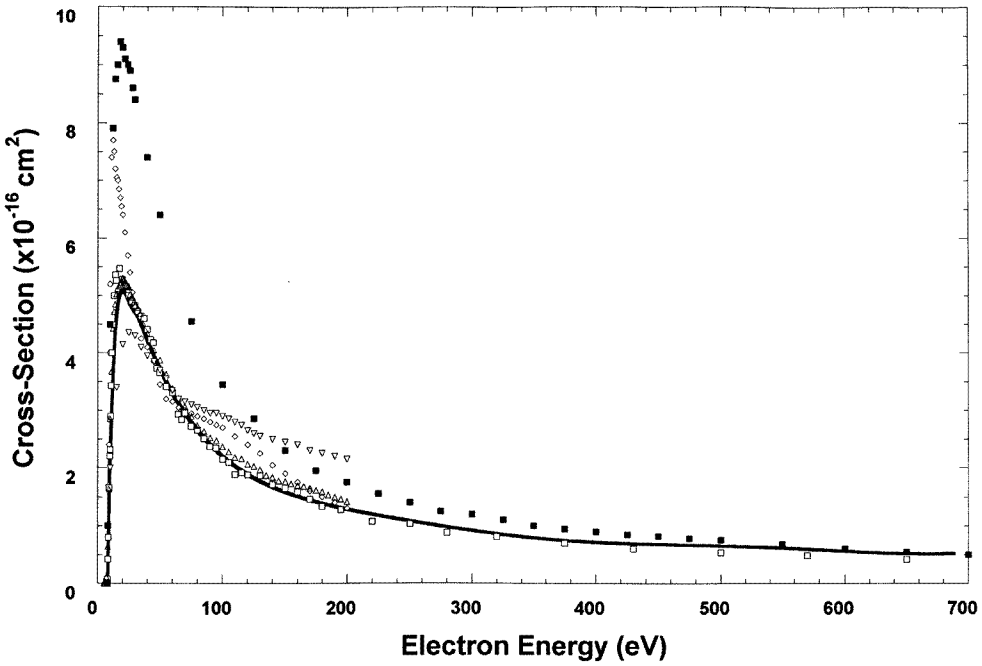

Figure 4. Single ionization cross section of Mg by electron impact. (——) Present data; (◊) Karstensen and Schneider (1978); (□) McCallion *et al* (1992); (△) Freund *et al* (1990); (▽) Vainshtein *et al* (1972); (■) Okudaira *et al* (1970).

measured by Okudaira *et al* (1970) for energies up to 1200 eV are compared to our results. At low energy (less than 200 eV) a poor agreement is found, their cross section values are systematically larger by a factor of 1.8 with respect to ours. At high energies (500 eV and higher), the agreement becomes increasingly better (13% and 7% difference at 500 and 600 eV, respectively).

The single-ionization cross section measurements by Karstensen and Schneider (1978) were performed from threshold to 200 eV. The overall agreement with our data is poor. At peak value their cross section is 50% higher than ours. Note also, that their cross section peak is located at 12 eV which is about 7–8 eV below the average peak energy measured by different experiments. This suggests an improper energy calibration or that their experiment is plagued with metastable Mg atoms which have a maximum ionization cross section at 13 eV (Shafranyosh and Margitich 1996). Only between 30 and 60 eV and for energy near 200 eV do the two cross section functions show a satisfactory match. Between 70 and 160 eV their cross section curve shows a bump not observed in our experiment. Although the cross sections measured by Vainshtein *et al* (1972) are really total ionization cross section, they may be compared to our present results. This is because their measurements were only made for energies up to 200 eV where single ionization is the dominant ionization process. At peak energy, their cross section is 15% smaller than ours and the general agreement is poor. The only satisfactory agreement is found in the 40–60 eV range. At higher energy (70–200 eV) the energy dependence of their cross section is quite different from what has been observed by our group and by others. Again, the cross section peak is observed at 25 eV which indicates a poor energy calibration.

For comparison purposes, all peak cross section values (experimental and theoretical)

Table 1. Cross sections for single, double and triple ionization of Mg by electron impact.

Electron energy (eV)	σ_1 (10^{-16} cm^2)	σ_2 (10^{-17} cm^2)	σ_3 (10^{-18} cm^2)
5.0	0.000		
10.0	2.100		
15.0	4.566		
20.0	5.080	0.000	
25.0	4.926	0.049	
30.0	4.731	0.124	
35.0	4.499	0.236	
40.0	4.232	0.324	
45.0	3.972	0.364	
50.0	3.733	0.385	
55.0	3.513	0.436	
60.0	3.312	0.538	
65.0	3.128	0.643	
70.0	2.959	0.745	
75.0	2.804	0.846	
80.0	2.663	0.944	
85.0	2.534	1.039	
90.0	2.416	1.131	
95.0	2.308	1.220	
100.0	2.209	1.306	0.000
110.0	2.037	1.467	0.011
120.0	1.893	1.614	0.030
130.0	1.771	1.747	0.057
140.0	1.669	1.865	0.089
150.0	1.582	1.969	0.126
160.0	1.507	2.059	0.169
170.0	1.441	2.136	0.216
180.0	1.383	2.202	0.267
190.0	1.330	2.256	0.321
200.0	1.282	2.301	0.376
225.0	1.175	2.374	0.519
250.0	1.080	2.406	0.657
275.0	0.994	2.411	0.781
300.0	0.916	2.400	0.885
325.0	0.848	2.382	0.966
350.0	0.792	2.360	1.022
375.0	0.748	2.337	1.055
400.0	0.716	2.313	1.070
425.0	0.693	2.286	1.071
450.0	0.677	2.255	1.064
475.0	0.664	2.219	1.052
500.0	0.650	2.178	1.038
525.0	0.633	2.132	1.023
550.0	0.612	2.085	1.008
575.0	0.587	2.039	0.990
600.0	0.560	1.997	0.967
625.0	0.535	1.959	0.937
650.0	0.518	1.919	0.904
675.0	0.513	1.862	0.877

and associated electron energy are shown in table 2. It is now apparent that the maximum value for single-ionization cross section is between 5.0 and 5.5×10^{-16} cm^2, and that this

Table 2. Comparison of cross section peak values for single ionization.

References	Peak cross section values (10^{-16} cm^2)	Energy at peak value (eV)
Experimental		
Present experiment	5.11	20.1
Shafranyosh and Margitich (1996)	5.0[a]	20.0[a]
McCallion *et al* (1992)	5.47	17.4
Freund *et al* (1990)	5.30	20.0
Karstensen and Schneider (1978)	7.70	12.0
Vainshtein *et al* (1972)	4.35	25.0
Okudaira *et al* (1970)	9.40	18.0
Theory		
McGuire (1977)	5.85	17.0
Modified Born, Peach (1970)	5.40	21.0
Born–Ochkur, Peach (1970)	4.6	20.0
Born-exchange, Peach (1966)	5.8	20.0
Coulomb–Born, Peach (1966)	6.9	20.0

[a] The ionization cross section has only been measured in the 0–21 eV range.

peak is located at about 20 eV. It is also clear, by looking at figures 3 and 4, that apart from absolute values at low energy, both the generalized oscillator strength approximation (McGuire 1977) and the modified Coulomb–Born (Peach 1970) are adequate to describe the energy dependence of the Mg ionization cross section.

3.3. Double-ionization cross section

Under the same conditions as described in the previous section, the double-ionization intensity $I_{Mg^{2+}}(E)$ is related to the double-ionization cross section $\sigma_{Mg^{2+}}(E)$ by the following expression:

$$I_{Mg^{2+}}(E) = K(m_{Mg^{2+}})G_{Mg}\sigma_{Mg^{2+}}(E) \tag{3}$$

where $K(m_{Mg^{2+}})$ is the combined transmission–detection factor for the doubly charged Mg ion. By dividing equation (3) by equation (2) and simplifying we obtain:

$$\sigma_{Mg^{2+}}(E) = \frac{I_{Mg^{2+}}(E)K(m_{Mg^{+}})}{I_{Mg^{+}}(E)K(m_{Mg^{2+}})}\sigma_{Mg^{+}}(E) \tag{4}$$

where the double-ionization cross section is now expressed in terms of the single-ionization cross section and of two ratios: intensity and combined transmission–detection efficiency. The first ratio can be obtained directly from the mass spectrum (see section 3.1), the second ratio, however, represents a more challenging problem. As is the case for most mass spectrometers, sensitivity depends on mass to charge ratio. To evaluate this K ratio ($K(m_{Mg^{+}})/K(m_{Mg^{2+}})$), we used a gas with similar fragment patterns and with well known single- and double-ionization cross sections. In the past, our group has performed a complete study of rare gas atoms by electron impact (Krishnakumar and Srivastava 1988). In this case, Ne (with observable fragments at 19.992, 9.996 and 6.664 amu closely compares to 23.985, 11.993 and 7.995 amu for Mg), is used to evaluate the K ratio. Rewriting equation (4) in terms of the neon K ratio, the Mg double-ionization cross section is given

by:

$$\sigma_{Mg^{2+}}(E) \approx \frac{I_{Mg^{2+}}(E)K(m_{Ne^+})}{I_{Mg^+}(E)K(m_{Ne^{2+}})}\sigma_{Mg^+}(E). \tag{5}$$

Intensity ratios are measured for Ne at different energies (100, 200, 300, 400, 500 and 600 eV) in the mass spectrum mode and used with the previously published cross sections (Krishnakumar and Srivastava 1988) to evaluate the K ratio value. A K ratio of 0.44 has been found in this case. A normalization factor is obtained by combining the K ratio values with the Mg ion intensity ratios measured in the mass spectrum mode (section 3.1). This factor is then multiplied by the single-ionization cross section at a specific energy, thus providing the absolute normalization factor for the double-ionization efficiency curve. The resulting cross section for double ionization is shown in figure 5. A curve fit has been performed on our experimental data and specific cross section values obtained from this fit are shown in table 1. The results of previous experiments are also shown in figure 5. Of particular interest is the 40–60 eV region, where a discontinuity in the cross section function can be seen. This discontinuity has been observed by both McCallion *et al* (1992) and Okudaira *et al* (1970) and has been interpreted to be due to the following Auger effect (Peach 1970):

$$Mg^+(2p^5 3s^2\ ^2P) \rightarrow Mg^{2+}(2p^6\ ^1S) + e^- \tag{6}$$

where this autoionization takes place immediately after removal of a 2p electron at 55.8 eV (Fiquet Fayard *et al* 1968, Slater 1955). Thus, two distinct processes are believed to contribute to the total double ionization cross sections: direct double ionization (which starts at 22.68 eV; Moore 1971) and Auger effect (which starts at 55.8 eV). As indicated by

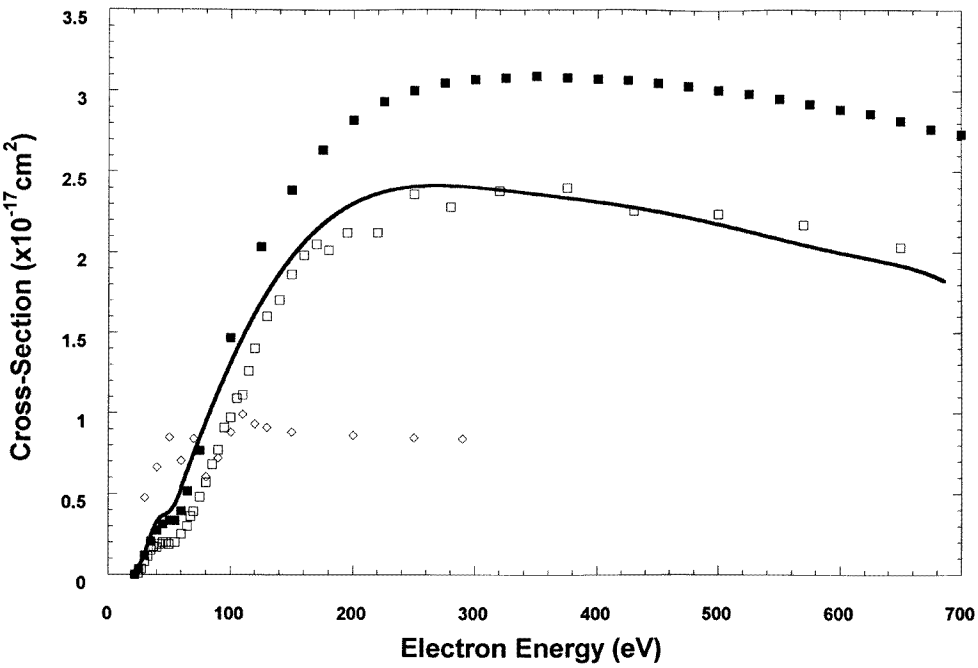

Figure 5. Double-ionization cross section of Mg by electron impact. (——) Present data; (◊) Karstensen and Schneider (1978); (□) McCallion *et al* (1992); (■) Okudaira *et al* (1970).

the smooth curve in figure 5, and confirmed by earlier measurements (Fiquet-Fayard *et al* 1968) the double-ionization process is, for energies higher than 60 eV, dominated by Auger processes. The fact that Auger double ionization is really a simple ionization (of an inner shell electron) followed by an autoionization also explains why the double-ionization cross section is unusually high compared to the single-ionization cross section. Although Auger effect involving the 2s inner shell (instead of the 2p) is clearly possible, this autoionization process, which requires an electron impact energy of at least 95.2 eV (Slater 1955), is not observed in our experiment (there is no discontinuity in the cross section between 90 and 100 eV). Thus, the cross section for Auger effect involving the 2s level is believed to be negligible with respect to the autoionization involving the 2p level. Double-ionization cross sections measured by McCallion *et al* (1992) are compared to the present values. A good agreement is found for electron energies higher than 100 eV. Note that their data exhibit a greater scatter than our measured cross sections. At low energy (20–40 eV), our cross sections are however about 40% larger than the values obtained by McCallion *et al* (1992). The double-ionization cross sections obtained by Okudaira *et al* (1970) are in reasonable agreement with the present values. At low energies, the agreement is good (within 10%) with both measurements showing the same Auger structure. At high energies, their cross section is about 33% larger than ours. Finally, cross sections measured by Karstensen and Schneider (1978) differ considerably from ours in both magnitude and energy dependence. The overall agreement with our data is very poor. Problems with their calibration technique and/or measuring procedure are suspected for this disagreement.

3.4. Triple-ionization cross section

In a similar fashion, the triple-ionization cross section for Mg is measured and normalized. In this case, we used, as described in the previous section, the K ratio $(K(m_{Mg^+})/K(m_{Mg^{3+}}))$ for singly and triply ionized Ne atom to normalize the triple-ionization efficiency curve obtained for Mg. Using equation (5), and rewriting it in terms of the triple-ionization cross section we have:

$$\sigma_{Mg^{3+}}(E) \approx \frac{I_{Mg^{3+}}(E)K(m_{Ne^+})}{I_{Mg^+}(E)K(m_{Ne^{3+}})}\sigma_{Mg^+}(E) \tag{7}$$

A K ratio of 0.36 has been found in this case. The resulting cross section for triple ionization is shown in figure 6. A curve fit has been performed on our experimental data and specific cross section values are shown in table 1. The results of previous experiments are also included in figure 6. The triple-ionization cross sections measured by McCallion *et al* (1992) are compared to our experimental values. The overall agreement is good. On average their cross sections are about 15% smaller than ours. Their data also exhibit a larger scatter than ours and fail to locate the threshold (102.8 eV, Moore 1971) for the triple-ionization process. The cross sections measured by Okudaira *et al* (1970) are in good agreement with present results. Their ionization efficiency curve is almost identical to ours and their absolute cross section values are on average only 7% higher than ours.

3.5. Discussion of errors

The uncertainties associated with single-, double- and triple-ionization cross sections are essentially composed of two independent sources: error related to the shape of the ionization efficiency curves and the error in the calibration factors used to normalize the curves. In all cases, the uncertainties related to the shapes of ionization efficiency curves are much

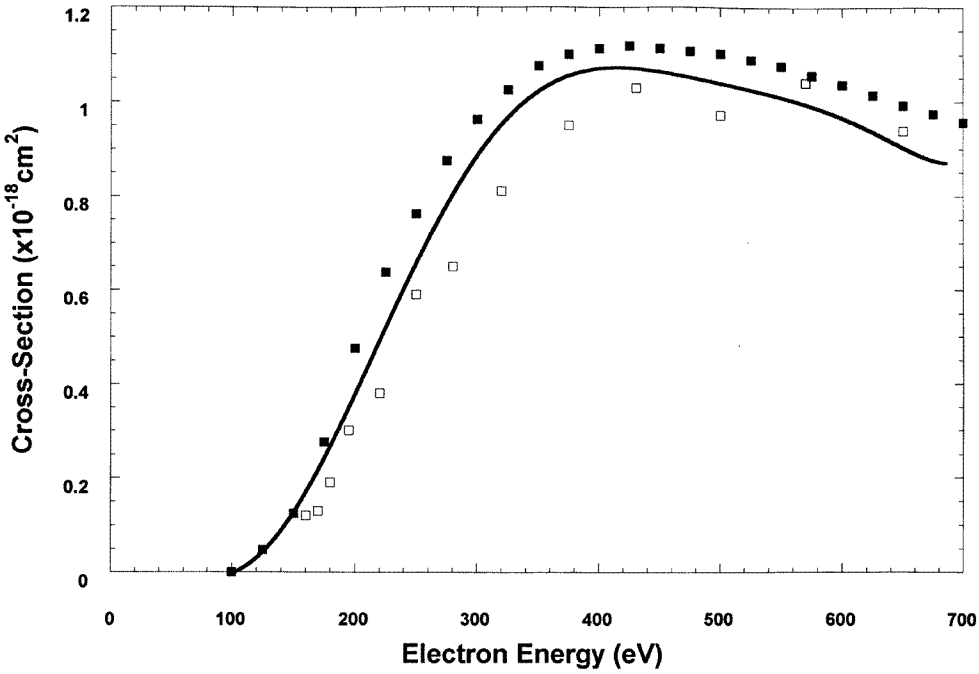

Figure 6. Triple-ionization cross section of Mg by electron impact. (——) Present data; (□) McCallion *et al* (1992); (■) Okudaira *et al* (1970).

smaller than the errors associated with the normalization. Thus, for all cross section curves, the error is essentially systematic and related to the absolute normalization procedure.

For single ionization, the principal source of error is the calibration factor used to normalize the ionization efficiency curve. In this case we used McGuire's (1977) calculations at 500 eV to normalize our curve. As mentioned earlier (see section 3.1) this model is believed to be very good to predict cross section at high electron energy. We assumed a ±10% error for this normalization factor and a ±3% error for the shape of the ionization efficiency curve (see section 2.2). This translates into a ±11% error bar for the single-ionization cross section. For double ionization, the resulting uncertainty must also include errors associated with the Ne single and double ionization used to evaluate the K ratio (see section 3.3). These errors have been evaluated previously (Krishnakumar and Srivastava 1988) and are ±10% and ±13%, respectively. The resulting uncertainty for double ionization is, therefore, estimated to be ±19%. Similarly, for triple ionization, errors associated with Ne single- and triple-ionization cross sections (±10% and ±22%, respectively) are included and, the resulting uncertainty is estimated to be ±25%.

4. Conclusion

Cross sections for single, double and triple ionization of Mg by electron impact have been measured in the 0–690 V range. For single ionization, a good agreement between these results and calculated cross sections using either the generalized oscillator strength approximation or the modified Coulomb–Born approximation is found. These results are

also in good agreement with the latest published cross sections. For double- and triple-ionization cross sections, reasonable agreements between these measurements and previously published cross sections are found.

Acknowledgments

The research reported in this paper was carried out at the Jet Propulsion Laboratory, California Institute of Technology under a contract with the National Aeronautics and Space Administration. RFB would like to thank NRC, Washington, DC, for a Resident Research Associateship grant during the course of this work.

References

Arnaud M and Rothenflug R 1985 *Astrophys. Suppl.* **60** 425
Brinkman R T and Trajmar S 1981 *J. Phys. E: Sci. Instrum.* **14** 245
Brooks E, Harrison M F and Smith A C H 1978 *J. Phys. B: At. Mol. Phys.* **11** 3115
Dunn G H 1985 *Electron Impact Ionization* ed T D Märk and G H Dunn (Berlin: Springer)
Feldman P D 1996 *Atomic, Molecular & Optical Physics Handbook* ed G W F Drake (Woodbury, NY: American Institute of Physics)
Fiquet-Fayard F, Chiari J, Muller F and Ziesel J P 1968 *J. Chem. Phys.* **48** 1478
Freund R S, Wetzel R C, Shul R J and Hayes T R 1990 *Phys. Rev.* A **41** 3575
Goodfellow 1997 *Technical Data Sheet*
Jefferies J T 1991 *Astrophys. J.* **377** 337
Karstensen F and Schneider M 1975 *Z. Phys.* A **273** 321
——1978 *J. Phys. B: At. Mol. Phys.* **11** 167
Khakoo, M A and Srivastava S K 1984 *J. Phys. E: Sci. Instrum.* **17** 1008
Krishnakumar E and Srivastava S K 1988 *J. Phys. B: At. Mol. Opt. Phys.* **21** 1055
Lotz W 1968 *Z. Phys.* **216** 241
McCallion P, Shah M B and Gilbody 1992 *J. Phys. B: At. Mol. Opt. Phys.* **25** 1051
McGuire E J 1977 *Phys. Rev.* A **16** 62
Moore C E 1971 *Atomic Energy Levels (NSRDS-NBS 35)* vol 1 (Washington, DC: US Govt Printing Office)
Okudaira S, Kaneko Y and Kanomata I 1970 *J. Phys. Soc. Japan* **28** 1536
Okuno Y, Okuno K, Kaneko Y and Kanomata I 1970 *J. Phys. Soc. Japan* **29** 164
Peach G 1966 *Proc. Phys. Soc.* **87** 375
——1970 *J. Phys. B: At. Mol. Phys.* **3** 328
Rao M V V S, Iga I and Srivastava S K 1995 *J. Geophys. Res.* **100** 421
Raymond J R and Smith B W 1977 *Astrophys. J. Suppl.* **35** 419
Rosenstock H M, Draxl K, Steiner B W and Herron J T 1977 *J. Phys. Chem. Ref. Data* Suppl 1 **6**
Shafranyosh I I and Margitich M O 1996 *Z. Phys.* D **37** 97
Shull J M 1982 *Astrophys. J.* **262** 308
——1985 *Electron Impact Ionization* ed T D Märk and G H Dunn (Berlin: Springer)
Slater J C 1955 *Phys. Rev.* **98** 1039
Srivastava S K and Nguyên H P 1987 *NASA/JPL Publication* No 87-2
Trajmar S, Williams W and Srivastava S K 1977 *J. Phys. B: At. Mol. Phys.* **10** 3323
Vainshtein L A, Ochkur V I, Rakhovskii V I and Stepanov A M 1972 *Sov. Phys.–JETP* **34** 271
Weast R C (ed) 1983a *CRC Handbook of Chemistry and Physics, Vapor Pressure of Elements* vol D-222 (Boca Raton, FL: Chemical Rubber Company)
——1983b *CRC Handbook of Chemistry and Physics, Table of Isotopes* vol B-258 (Boca Raton, FL: Chemical Rubber Company)